

Protein reconstitution into freestanding planar lipid membranes for electrophysiological characterization

Thomas Gutschmann¹, Thomas Heimburg², Ulrich Keyser³, Kozhinjampara R Mahendran⁴ & Mathias Winterhalter⁵

¹Research Center Borstel, Center for Medicine and Bioscience, Division of Biophysics, Borstel, Germany. ²Membrane Biophysics Group, Niels Bohr Institute, University of Copenhagen, Copenhagen, Denmark. ³Cavendish Laboratory, University of Cambridge, Cambridge, UK. ⁴Department of Chemistry, University of Oxford, Oxford, UK. ⁵Jacobs University Bremen, Bremen, Germany. Correspondence should be addressed to M.W. (m.winterhalter@jacobs-university.de).

Published online 31 December 2014; doi:10.1038/nprot.2015.003

The reconstitution of channel-forming proteins into planar lipid bilayers enables their functional characterization at very low (sometimes below attomolar) concentrations. We describe the three main approaches used in our laboratories (the Mueller-Rudin technique, in which the bilayers contain an organic solvent, the Montal-Mueller or solvent-free technique, and a method for membrane reconstitution via liposome formation), and we discuss their respective advantages and limitations. Despite the differences in the reconstitution procedures, subsequent protein characterization is based on the same electrophysiological technique. A transmembrane electric field is applied, inducing an ion current and allowing conclusions to be drawn on apparent pore sizes, or suggesting functional properties such as channel opening and closing upon ligand binding, pH-induced conformational changes, ion selectivity or substrate specificity.

INTRODUCTION

Cell walls allow selective permeation of nutrients or signaling compounds while protecting the interior from substances that are toxic to cells. Investigation of their permeability is fundamental for the understanding of cellular function, and whole-cell permeability assays might give answers to questions about biological phenomena. In general, the cell walls have a complex structure that contains one or more lipid membranes and polymer layers. To gain an understanding of the underlying molecular mechanism of permeability, it is necessary to reduce the number of parameters involved. In general, the lipid membranes with embedded channel-forming proteins are the typical selective filter for hydrophilic small molecules. One class of membrane gates are water-filled channel-forming proteins that allow ions and hydrophilic molecules to cross the membrane^{1–3}. However, to date, there is no general direct method to determine the rate at which small molecules move through single protein channels, as all methods for detecting the flux require the signal to be amplified.

Signal amplification in electrophysiology is based on differences in conductance: the lipid membranes are almost perfect insulators, and thus the presence of even a single conducting channel in a 1-mm² large lipid membrane is readily detected^{1,4–13}. This extreme contrast in conductance makes electrophysiology the most suitable method for detecting minor changes in membrane conductance: patching a piece of cell membrane with a pipette and recording the ion current across the membrane provides information on channel structure, ion selectivity, channel conformation changes or on the passage of uncharged molecules^{4–13}. However, not all cells can be patched. Typically, bacteria are too small, and, moreover, they contain lipopolysaccharides (LPSs), a polymer layer that inhibits the formation of an electrically tight seal.

Fifty years ago, Rudin and co-workers⁵ presented a method known as black lipid membranes (BLMs) to characterize the physicochemical properties of lipid membranes. Lipids extracted from natural membranes were used to form 6–9-nm-thick and 10-mm² large patches across an orifice. Limited by a lack of

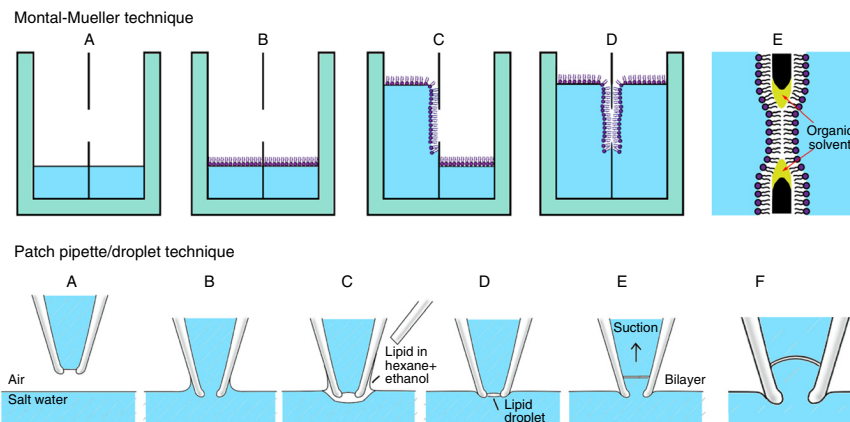
precise knowledge of membrane proteins, early investigations reported only on electrical properties of ‘membrane active components’⁵. In the following decade, this technique was refined and applied to characterize the electrical properties of lipid membranes, including membrane dielectric constants, surface charge or inner membrane potentials^{14–16}. Moreover, nowadays substantially more information on membrane proteins is available, and their reconstitution into planar lipid bilayer contributes enormously to our understanding of their function. Even without knowing the structure of the protein, using only a tiny amount of material in planar lipid bilayer experiments provides crucial preliminary information on the size of a channel and its functional characteristics^{8–10}. Typical channel-related questions for which electrophysiology provides an answer concern the potential channel size and surface charge or binding sites inside the channel. Other questions can be answered by experiments involving target channel gating induced by voltage, pH, mechanical stress or ligand binding.

Overview of approaches used in our laboratories

The first method suggested by Mueller *et al.*⁵ was the so-called solvent-containing membrane, and it is detailed in Step 1A of the PROCEDURE. Here the lipids are dissolved in an organic solvent, typically decane, and they are painted across a small circular hole^{5,9}. These solvent-containing membranes appear to be soft and flexible. This method is recommended when the aim is to elucidate the potential channel-forming activity of uncharacterized proteins (or peptides). The presence of hydrophobic solvent inside the lipid bilayer allows one to adapt the hydrophobic thickness of the membrane thickness and thus to match the hydrophobic part of the protein. Thus, it simulates a broad spectrum of possible natural membranes.

In a second so-called solvent-free method suggested by Montal and Mueller⁶, the lipids are spread with an organic solvent on top of the aqueous buffer. This is described in Step 1B of the PROCEDURE. The Montal-Mueller technique (**Fig. 1**, top)

Figure 1 | Two methods for forming lipid membrane patches. Top, the Montal-Mueller technique generates a membrane patch over a hole in a Teflon film in a series of steps (A–E)⁶. Typical diameters of the membrane patch are in the range of 50–100 μm . Bottom, the patch pipette technique (steps are labeled A–F) generates a membrane over the tip of a patch pipette that is in contact with a water surface. The typical membrane patch diameter is 1–10 μm (refs. 17,18).

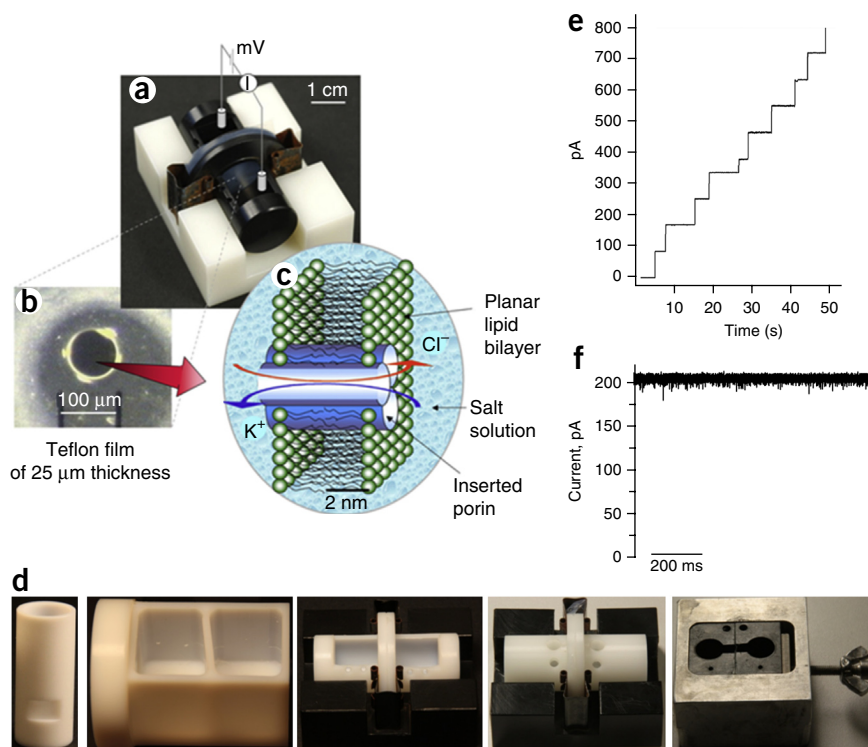


generates a lipid bilayer from two monolayers (BLM) over a Teflon hole with a diameter in the range of 50–100 μm . To reduce monolayer stress at the edges of the Teflon hole, the edges of the hole are pre-painted with an organic solvent, such as hexadecane. The hole in a Teflon foil can also be replaced by patch pipettes^{17,18}. For this, a droplet of lipid in organic solvent (e.g., a hexane/ethanol mixture) is brought in contact with the outer surface of a patch pipette (diameter 1–10 μm) that barely touches an aqueous surface (Fig. 1, bottom). Solvent-free membranes are also known as folded membranes, as they are created out of two monolayers. In most cases, symmetric membranes are used, in which lowering and raising the water level below the lipid monolayer allows rapid membrane formation. The great advantage of this technique is the control over the content of each lipid monolayer. This gives the possibility to form an asymmetric membrane by spreading a second lipid composition on the other compartment and by raising both water levels after spreading the lipids¹⁰. This is described in Step 1C of the PROCEDURE.

Surprisingly, the asymmetry is maintained even if the bilayer is re-formed after rupture.

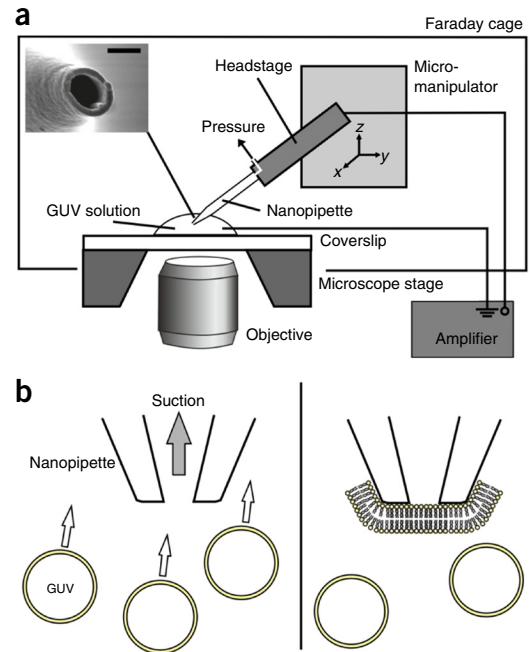
Independently of the above-described bilayer formation technique, the starting point for channel reconstitution is similar (Fig. 2; Step 2 of the PROCEDURE): reconstitution is usually initiated by adding very small amounts of protein stock solutions containing a detergent at a concentration that is above the critical micellar concentration (CMC). If the protein solution is then rapidly diluted below the CMC of the detergent, this increases the likelihood that the membrane protein will denature, precipitate or aggregate. Therefore, only a single protein or a few proteins need to reach and be inserted into the membrane. Achieving single-channel reconstitution experimentally seems to be a question of which kinetic wins, reaching the membrane versus aggregation. Single-channel reconstitution is reproducibly

Figure 2 | Typical experimental bilayer setup. (a) Two Delrin half-cells sandwich a Teflon foil. (b) Microscopic image of the hole in the Teflon foil. Note that to achieve a stable bilayer coating, the hole in the Teflon should be perfectly round without halos. (c) Schematic view of a bilayer lipid membrane with a trimeric channel inserted. Depending on the applied transmembrane voltage, anions and cations are pulled into the respective half-cell. (d) Typical chambers used in our laboratory. Left, a round Teflon piece is machined to have a thin remaining layer that allows punching a hole in the thinnest part. This cell can be placed in any other cuvette hosting the ground electrode. The second chamber is a complex one-piece cuvette. On one side it contains a glass window to optically follow the formation of a black film. The separating wall is slightly tilted to avoid light reflection from the Teflon edge. The chamber in the middle contains two half-cells to sandwich a Teflon foil. The same cuvette can be made with a smaller volume (200 μl). Right, we show a cuvette with an aluminum block devoted to be coupled to a Peltier element for temperature regulation. (e) Multiple OmpF channel insertions in solvent-containing membranes at 1 M KCl, 20 mV (pH 6). (f) Ion current recordings through single OmpF channel in solvent-free lipid bilayer at 1 M KCl (pH 6) at an applied voltage of 50 mV. Images in e,f provided in-house (Jacobs University Bremen) by I. Barcena Urbarri with permission.



PROTOCOL

Figure 3 | Adapted patch-clamp setup for the formation of small lipid bilayers on nanopipettes¹². (a) A nanopipette is dipped into a small droplet of GU solution. The inverse microscope is used to follow the formation process and to image lipid buildup on the nanopipette. Pressure is applied with a syringe at the inlet of the pipette holder mounted on the amplifier headstage. The upper left inset shows a SEM image of a typical nanopipette; scale bar, 200 nm. (b) Sketch of the formation process shows GUVs in solution that are sucked toward the opening; upon contact, one bursts and blocks the hole with a lipid double layer (not drawn to scale). There is no need for approaching or catching the GUVs, as the whole process works with applied suction to the pipette tip.



obtained by optimizing the dilution of the protein stock solution. Depending on the type of lipid membrane, the observed reconstitution kinetics are very different. Obviously, the larger the lipid membrane area is, the higher the probability that a protein will be incorporated. Our experimental observations (M.W., unpublished observations) suggest that solvent-containing membranes appear to promote protein reconstitution.

A third approach (Fig. 3) is to reconstitute channel-forming proteins first into liposomes and to aspirate the giant liposomes using patch pipettes^{11,12}, solid-state nanopores¹³ or glass chips¹⁹. This is described in Step 1D of the PROCEDURE. Glass nanopipette tips are very promising supports for single-molecule studies with protein channels, owing to their ease of fabrication and easily controlled diameters down to 200 nm (refs. 12,18,20–22). Glass nanopipettes can be fabricated simply by drawing glass capillaries in a standard pipette puller in a matter of minutes. When they come in contact with the tip of the glass pipette, giant unilamellar vesicles (GUVs) containing cholesterol in their membranes break, forming a single-lipid double layer. This straightforward and easy-to-learn method reliably forms supported bilayers with areas down to $4 \times 10^{-14} \text{ m}^2$. Surprisingly, this process works without modification of the glass, and it allows for relatively rapid formation of tens of bilayers from individual GUVs on the same nanopipette.

Applications

Our expertise lies mainly in the characterization of bacterial porins, and we used this technique to elucidate pore size or selectivity for ions^{23,24}. Moreover, we are interested in permeation of solutes across bacterial channels^{25–30}. For this, in contrast to ions, the transport of uncharged compounds does not contribute directly to the conductance. However, the presence of uncharged molecules in a membrane channel may cause detectable fluctuations of the

ion current. These substrate-induced fluctuations have been used to quantify translocation of molecules through channels.

Electrophysiology is able to detect low ion currents down to $\sim 1 \text{ pA}$ ($1 \text{ pA} = 6 \times 10^6$ elementary charges/s), and it determines the time resolution of the recording system. In the complete absence of proteins, the synthetic lipid membrane itself can display ion channel-like events that are very similar to or even indistinguishable from protein channel traces (an example is shown in Fig. 4)³¹. The open probability of the channels is voltage-gated (Fig. 4, bottom right), whereas the single-channel conductance is constant (linear I - V profile, Fig. 4, top right). The first reports of such lipid pores stem from the early 1980s (ref. 32), and they were extensively reviewed by Heimburg and colleagues^{33–36}. It has been found^{31,32} that lipid channels can also be gated by temperature changes, and that they can be inhibited by general anesthetics. It seems likely that proteins can facilitate lipid pore formation via their influence on lipid phase behavior³⁴. These lipid channels are caused by thermal density fluctuations in the membrane that are close to the melting transition of the lipid membranes, which may exist in biological membranes, ~ 10 – 20°C below physiological temperature. Any change in a thermodynamic variable that alters phase transitions might modify the occurrence of lipid channels. Thus, besides being voltage-gated and temperature-sensing, the lipid channels are mechanosensitive, and they are gated or inhibited by drugs such as general or local anesthetics, or they can be gated by calcium. Note that the observed conductance modulations (Fig. 4) are similar to those found for protein channels.

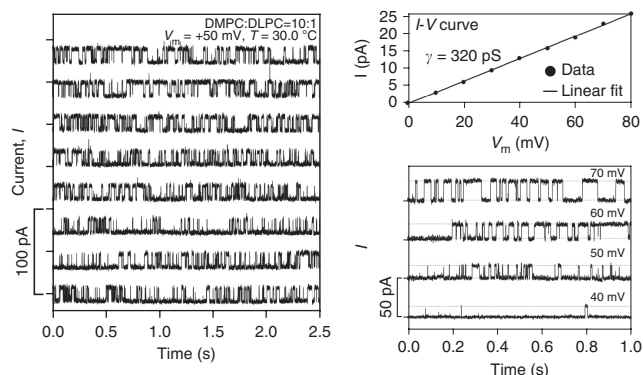


Figure 4 | Lipid ion channel events in a synthetic lipid membrane made of a mixture of di-myristoyl-phosphatidyl-choline (DMPC) and di-lauroyl-phosphatidyl-choline (DLPC) in a 150 mM NaCl solution. Left, ion current traces (reproduced from ref. 31, with permission from Elsevier). Right, ion current trace analysis. The open probability of the channel is voltage-gated (bottom right), whereas the single-channel conductance is constant (linear I - V profile, top right). (Right-side images are reproduced from ref. 36 under the terms of a Creative Commons Attribution licence.)

Future technical developments are miniaturization of the membrane; in addition to the enhanced mechanical stability, smaller membranes reduce the total capacitance and thus allow faster recordings. Combining the results from electrophysiology with those from all atom molecular modeling allows a molecular

interpretation of the protein function. The current all-atom computer simulations reach the upper-nanosecond range and are now able to predict astonishing ion conductances. The use of refined sampling algorithms allows one to suggest the most likely pathways of larger substrates across the channel.

MATERIALS

REAGENTS

▲ **CRITICAL** Doubly distilled and deionized water should be used to prepare all aqueous solutions. After preparation, all solutions should be purified by filtration through a 0.4- μm filter.

Buffer components

- HEPES
- MES
- TRIS
- Potassium phosphate (recommended for temperature measurements)
- Potassium chloride

Detergent

- Octyl-polyoxyethylene (OPOE), Alexis

Reagents for preparing solvent-containing membranes (Step 1A)

- For cleaning: acetone, KOH, isopropanol
- Typical solvents: n-decane, chloroform
- Pre-painting solution: dissolve lipids, such as DPhPC (1,2-diphytanoyl-sn-glycero-3-phosphocholine; DPhPC (Avanti Polar Lipids, cat. no. 850356P), in volatile solvent, e.g., chloroform (1 wt%). This stock solution can be applied directly or it can be stored at $-20\text{ }^{\circ}\text{C}$ for longer periods (6 months)
- Membrane-forming solution: dissolve DPhPC in decane (1 wt%). This stock solution can be applied directly or it can be stored at $-20\text{ }^{\circ}\text{C}$ for longer periods (6 months)

Solvent-free membranes (Montal-Mueller; Step 1B)

- Typical solvents: hexadecane, pentane, hexane and squalene
- Pre-painting solution: use a volatile hydrocarbon such as pentane to dissolve long-chain alkanes. 1 wt% hexadecane in pentane works well. In contrast, low-temperature measurements require 2 wt% squalene in pentane. This stock solution can be applied directly or it can be stored at $-20\text{ }^{\circ}\text{C}$ for longer periods (6 months)
- Membrane-forming solution: dissolve lipids, DPhPC usually works best, in pentane/hexane (1 wt%). This stock solution can be applied directly or it can be stored at $-20\text{ }^{\circ}\text{C}$ for longer periods (6 months)

Glass nanopipette bilayers (Step 1D)

- Cholesterol (Sigma-Aldrich, cat. no. C8867)
- Bio-beads SM2 (Bio-Rad, cat. no. 152-3920)
- Sorbitol
- Lipid-containing solution, 10 mM DPhPC with up to 10 mol% cholesterol (mole/mole), dissolved in chloroform ▲ **CRITICAL** 10 mol% cholesterol is important to get stable lipid bilayers.

EQUIPMENT

- Teflon foil of 25- μm thickness (Goodfellow Cambridge)
- High-voltage discharge BD10A (Electrotechnic Products)
- Axopatch 200B amplifier (Axon Instruments)
- Axon Digidata 1440A digitizer and analysis program (Clampfit)
- HCC-100A temperature controller (Dagan)
- Borosilicate glass capillaries (Hilgenberg)
- Laser pipette puller (P-2000, Sutter Instruments)
- Ag/AgCl electrodes (World Precision Instruments or custom-made electrodes)
- Indium tin oxide (ITO)-coated glass slides
- Faraday cage setup
- Micromanipulator for pipettes

REAGENT SETUP

Lipids The most widely used lipid for planar lipid membranes is DPhPC in powder (DPhPC is obtained from Avanti Polar Lipids). DPhPC has ideal bilayer-forming properties. It exists in the fluid lamellar phase across a wide temperature range (-120 to $+120\text{ }^{\circ}\text{C}$; ref. 37), and it is stable to oxidation. Other lipids can be used (e.g., α -lecithin or egg-PC, which are mixtures of components extracted from natural membranes). These other lipids work fine for reconstitution of membrane proteins, but they open the question of

whether possible components of the heterogeneous rather undefined lipid mixture might be interacting with channels. Other natural or artificial homogeneous lipid compositions can be used, but the researcher should be aware of some of the difficulties in forming stable membranes and resistance to protein reconstitution.

Potassium chloride Typically, lipid bilayer experiments are carried out with 0.01–3 M potassium chloride (KCl). The dominant choice of KCl is because of the similar electrophoretic mobility of both the cation and the anion. We typically use 1 M KCl (analytical grade, from Sigma-Aldrich), depending on the desired pH additional buffer components added. An example buffer for a typical measurement would have the following composition: 1 M KCl (high conductance of the buffer allows the detection of small channels or small changes in the size of the channel) and 10 mM Tris buffer. An example buffer for use in temperature measurements would have the following composition: 1 M KCl and 10 mM potassium phosphate, as the buffering property is relatively constant for this buffer. These buffers can be stored at $4\text{ }^{\circ}\text{C}$ for a few days.

EQUIPMENT SETUP

▲ **CRITICAL** A very good introduction to electrophysiology can be found in the book by Sakmann and Neher⁴, which contains the underlying theory as well as a collection of technical problems and their solutions.

Bilayer chambers We typically use custom-made vertical bilayer chambers made from Teflon or Delrin with a wide variety of shapes and solution volumes ranging from 200 μl to 2 ml. In **Figure 2**, we show a number of chambers that are used in our laboratory. Commercial options are also available (e.g., from Warner Instruments). Common to all is the necessity to separate two chambers, which allows a small gap in the separation that can be spanned by a bilayer lipid membrane⁵. Solvent-containing membranes are painted across the Teflon orifice. By using this technique, it is possible to cover larger areas (1 mm^2). Solvent-containing membranes have the tendency to clog small holes; therefore, it is better to use chambers with larger holes (i.e., $<500\text{ }\mu\text{m}$) for solvent-containing membranes. It is interesting to note that some years ago the stability of various pore geometries was investigated, and the optimal ratio of holding wall thickness to pore size was found to be 1:10 (ref. 38). Lowering or raising of folded membranes (i.e., for the procedures in Step 1B) means that large holes cannot be coated, and the deficit in solvent prevents clogging to some extent. Subsequently, this technique is suitable for smaller holes^{1,5,6}. Solvent-containing membranes allow the formation of large membranes, and thus it can be made across thick Teflon separation that can be obtained by machining permanent holes out of a Teflon block. It is better to make solvent-free membranes by punching holes into thin polytetrafluoroethylene (PTFE) Teflon foils. Holes can be readily punched in a Teflon foil of 25- μm thickness by a high-voltage discharge BD10A. The discharge melts the edge of the Teflon foil. The hole that is devoted to carry the membrane patch has to be adapted to the type of membrane to be formed. For example, in the case of temperature measurements, we use Teflon film with a hole of 40- to 50- μm diameter. The two halves of the bilayer chamber are fastened together with silicone glue and the PTFE film of $\sim 40\text{ }\mu\text{m}$ aperture across which the bilayer is formed.

A standard cleaning routine is used for cleaning the chambers: first, rinse with large amounts of distilled water, followed by an acetone wash. Finally, the chambers are thoroughly dried under a stream of nitrogen. When required, we also use KOH (3 M) and isopropanol washes to remove proteins.

Current amplifier The core of all approaches is the current amplifier. Several options are available, depending on the budget and desired time resolution. The chosen equipment often includes a dedicated AD/DA converter and software for data analysis.

We use mostly Axopatch 200B amplifier together with Axon Digidata 1440A digitizer and analysis program (Clampfit) for the signal recording and

PROTOCOL

analysis on a standard PC. We perform our measurements in a voltage-clamp mode using resistive whole-cell ($\beta = 1$) headstage settings. The Axopatch 200B amplifier has a recording bandwidth of 100 kHz, and the digitizers have a maximum sampling rate of 250 kHz per channel, which determines the maximum temporal resolution (4 μ s).

Electrical recording experiments should be carried out in a Faraday cage to shield from external electrical noise. We use a homemade steel box that is grounded through the common ground in the amplifier.

For temperature measurements, we include a HCC-100A temperature controller (Dagan), which does not introduce electrical noise into measurements. In the temperature system, heating and cooling are controlled by the use of Peltier devices. However, any other system for temperature control should work as well^{27,39}.

Electrical connections The electrical connection between the amplifier and the bath are typically Ag/AgCl electrodes (World Precision Instruments or custom-made electrodes). In some cases, for smaller cuvettes, thin silver wires can be used. These wires have to be treated often with bleach (any commercially available liquid bleach is suitable), or they can be activated in KCl solution. Particular care has to be taken with respect to electrode

resistance and possible electrolyte effects at the electrode. The use of a 3 M KCl/agar bridge between an electrode and the chamber solution is recommended for experiments carried out under asymmetric salt conditions to reduce potential offsets.

Electrodes for GUVs for protein reconstitution and glass nanopipette bilayers The electrodes are formed by transparent ITO-coated glass slides (52 \times 29 mm) with an SiO₂ passivation layer between the ITO layer and the glass substrate and a typical ohmic resistance of $\leq 10 \Omega$ (R_{sq}). The use of transparent electrodes allows the whole process to be observed through phase-contrast microscopy. The GUVs can be prepared using the electro-formation method, by spreading lipids in volatile solvent on a lipid glass slide. This can be easily self-made using a polydimethylsiloxane (PDMS) spacer. More sophisticated instruments include the GUV chamber connected to the Nanion Vesicle Prep Pro setup. Similar results can be obtained by using ITO glass slides and connecting them to a function generator. The underlying technique consists of applying an AC field, which is used to rehydrate a dry lipid film⁴⁰.

Capillaries for glass nanopipette bilayers Borosilicate glass capillaries (Hilgenberg) are used, and pipettes are prepared by drawing the glass capillaries with a laser pipette puller (P-2000, Sutter Instruments).

PROCEDURE

1| Follow one of the four main procedures to form a planar bilayer. Option A describes how to prepare a solvent-containing membrane for easy protein reconstitution (to characterize new protein). Options B and C describe how to prepare a solvent-free membrane for single-channel reconstitution and stochastic sensing of small molecules (can be used for experiments that take several hours). Option C should be chosen if you want to prepare asymmetric membranes (for example, LPS on one side and lipid on the other side). Option D describes how to prepare glass nanopipette bilayers, allowing the formation of extremely stable membranes (e.g., they allow the application of up to 600 mV without breaking). In comparison with option A, options B and C require more experimental patience with respect to protein reconstitution. Option D is technically more demanding.

The Montal-Mueller method (option B) for preparing solvent-free membranes allows more complexity with respect to membrane formation: For example, instead of lipids a fraction of LPS can be added^{10,30}. By using option C, we have been able to create an artificial bacterial outer membrane that has deep rough mutant LPS on one side, and on the other side it has a mixture of phosphatidylethanolamine from *Escherichia coli*, phosphatidylglycerol from *E. coli* and cardiolipin (diphosphatidylglycerol), with the phosphatidylethanolamine/phosphatidylglycerol/diphosphatidylglycerol ratio being 81:17:2 (refs. 10,30). The solvent-free bilayers typically have lifetimes of a few hours, and they can withstand constant applied potentials of 300 mV; asymmetric lipid membranes appear less stable.

(A) Solvent-containing membranes (Mueller-Rudin) ● TIMING 1–2 h

- (i) Pre-painting of the cleaned and dry Teflon chamber: smear $\sim 1 \mu$ l of the pre-painting solution on each side, and allow the solvent to evaporate for ~ 20 min.
- (ii) Fill the chamber with electrolyte buffer.
- (iii) Add $\sim 1 \mu$ l of the membrane-forming solution on a Teflon loop, and use this loop to smear it across the hole in the Teflon chamber likewise forming a soap film.
- (iv) Allow the multilayer to thin out for a few minutes; application of short (< 1 ms) voltage pulses will help squeeze the solvent out.
- (v) The quality of the bilayer formation can be followed optically using a low-amplification microscope. The initial multilamellar membrane across the hole shows colorful light reflection from the membrane, which indicates a film thickness that is above the wavelength of light. The formation of a bilayer turns the reflecting light into a gray spot (BLM).
- (vi) Determine the quality of the membrane electrically: for example, the application of a triangular voltage ramp will cause a rectangular capacitive current of $I = C \times dV/dt$, where V stands for the applied voltage. An applied triangular voltage waveform produces a square-wave current output ($dV/dt = \text{constant}$, for each sweep), which can be used to determine bilayer capacitance. Calculate the capacitance C from the height of the rectangular pulse. The lipid bilayer area is obtained using the approximation of a plate condenser $C = \epsilon_{\text{lipid}} \epsilon_0 A/d$, where ϵ_{lipid} is the relative dielectric constant of the lipid hydrocarbon (~ 2), $\epsilon_0 = 8.85 \times 10^{-12}$ As/Vm is the dielectric constant of the empty space, A is the area of the membrane and $d = 4\text{--}6$ nm is the hydrophobic thickness of the membrane.
At this point, you should expect that a free-standing lipid bilayer of $\sim C = 1$ nF capacitance corresponding to ~ 1 mm² area has formed. The solvent-containing bilayers typically have lifetimes of a few hours after formation, and they can withstand constant applied potentials of 50–100 mV.
- (vii) Reconstitute the protein channels, as described in **Box 1 (Fig. 2b)**.

? TROUBLESHOOTING

Box 1 | Protein reconstitution into planar membranes ● TIMING 30 min

Additional materials:

Protein: For our studies, we use mostly porins that we extracted ourselves from the outer cell wall of *E. coli*, in particular OmpF, which is well known for its stability⁶⁰. Typically, bacterial porin stock solutions are kept at 4 °C at a 1 mg/ml concentration in detergent solution above the CMC^{61,62}. Many other proteins require –80° or –20 °C with limited shelf life, depending on the type of channel degradation observed within a few days up to 20 years. Degradation is typically seen as additional noise in the conductance.

Preparation of a diluted protein stock: Dilute the protein into a detergent-containing solution and vortex it for a few seconds. The optimal dilution depends on the type of protein. Often, reconstitution works substantially better at higher dilution, e.g., lower than 0.1 mg/ml of protein, typically dissolved in 1 wt% OPOE.

Procedure

1. Add a small amount of protein, i.e., <1 µl (at 0.1 mg/ml), into the chamber. The protein would typically be a porin. Stirring and/or application of a voltage pulse (200 mV) might help the protein to reach the membrane. Depending on the type of membrane, size and shape of the cuvette, detergent or protein should reach the membrane after a few minutes, causing spikes in the ion current. The perfect insertion should be seen as current steps (**Fig. 2e**). In solvent-containing membranes, we expect a rapid insertion of single channels up to a few thousand within 10–60 min. Often, after 30–60 min, the protein insertion slows down and reaches a final value of conductance.

2. To achieve single-channel protein reconstitution in the solvent-free membrane, add the protein at a low concentration (final concentration: nanomolar to attomolar, typically picomolar to femtomolar) and perfuse to remove free protein from the bulk solution once a single pore has been inserted.

▲ **CRITICAL STEP** It is best to perform the insertion at 25 °C (ref. 27).

? TROUBLESHOOTING

(B) Solvent-free membranes (Montal-Mueller) ● TIMING 1–2 h

(i) Pre-painting of the cleaned and dry Teflon cuvette: smear ~1 µl of the pre-painting solution on each side of the Teflon hole, and allow the solvent to evaporate for ~5 min. Too much will clog the hole, and too little will not allow membrane formation.

▲ **CRITICAL STEP** The Teflon holes should be viewed using a light microscope for accurate pre-painting of the hole.

▲ **CRITICAL STEP** In the case of low-temperature measurements (i.e., <20 °C), the pre-painting should be done with 2 wt% squalene^{27,39}. A different solvent is necessary to avoid phase transition. Fill the chamber with buffer.

(ii) Spread ~10 µl of the membrane-forming solution on top of the buffer. Note that the amount of lipid required depends on the cuvette air-water interphase; typically, the area of the spread lipid should correspond to a few lipid layers (count ~0.6 nm² per lipid molecule).

(iii) The final control is performed by a similar procedure as for Mueller-Rudin. Free-standing lipid bilayer of $\sim C = 0.1$ nF capacitance corresponds to an area of ~10⁻¹ mm². The solvent-free bilayers typically have lifetimes of a few hours, and they can withstand constant applied potentials of 300 mV.

(iv) Reconstitute the protein channels as described in **Box 1** (refs. 25–30; **Fig. 2c**).

? TROUBLESHOOTING

(C) Variation of the Montal-Mueller procedure to prepare asymmetric membranes ● TIMING 1–2 h

(i) Pre-paint a clean, dry Teflon cuvette, as described in Step 1B(i).

(ii) Cover the bottom of each compartment with ~100 µl of the desired buffer.

(iii) Spread on each side ~10 µl of the respective membrane-forming solution on top of the buffer.

(iv) Add the remaining buffer needed to fill the chamber volume to create the first monolayer; complementation of the buffer into the second compartment should result in a complete bilayer.

(v) Reconstitute the protein channels as described in **Box 1**.

▲ **CRITICAL STEP** This procedure allows the formation of asymmetric membranes; in the case of unsuccessful formation or rupturing, Step 4 can be repeated. It is important to note that both membranes seem not to mix.

(D) Formation of free-standing lipid bilayers on glass nanopipettes ● TIMING 1–2 h

(i) Before use, thoroughly clean the capillaries by sonication in acetone and ethanol for 5 min, respectively. Remove residual ethanol from the cleaning process with gaseous nitrogen.

(ii) Mount the capillary glass in the laser pipette puller, in which the glass is heated and pulled to form two virtually identical pipettes. Tune the parameters of the pull, such as temperature and velocity, to optimize the tip opening and the length of the conical glass part. The parameters have to be adapted to each individual pipette puller.

PROTOCOL

An exact guideline of how to obtain the optimal pipette shape is beyond the scope of this protocol, but it can be found on the webpage of Sutter Instruments (http://www.sutter.com/PDFs/pipette_cookbook.pdf).

▲ **CRITICAL STEP** Keep an eye on the pulling times of the pipette puller during fabrication. If the times are changing markedly from run to run, then there might be a problem with the heating source, either laser or filament. Repair the pipette puller and start by characterizing the nanopipette openings again.

- (iii) To determine the shape and diameter of the tip, image the pipettes using scanning-electron microscopy (SEM). In Step 6, the current-voltage characteristics for each imaged pipette will be recorded to have an expectation value for good membranes. This calibration process allows for the determination of the tip diameters from simple ionic current measurements without the need for constant SEM monitoring. Repeat this calibration process after introducing a new batch of glass or a new pipette puller.
- (iv) Mount the nanopipettes onto a standard electrophysiology amplifier (e.g., Axopatch 200B, Molecular Devices) that is fixed to a commercial micromanipulator (e.g., Scientifica, PatchStar PS-7500). This should be done on an inverted microscope to allow for imaging of the bilayer formation process (**Fig. 3**).
- (v) Add measurement buffer to the top of a microscope slide. Minimize the volume by adding only a few tens of microliters. This forms the bath solution for the measurements.
- (vi) Move the nanopipette, filled with the same measurement buffer, into the bath solution using the micromanipulator. Characterize the nanopipette by measuring the current-voltage characteristic to determine the diameter using the calibration.

Box 2 | GUV formation and reconstitution of membrane proteins into giant vesicles for patch clamping ● **TIMING 1–2 h**

One way to overcome the tedious procedure of protein reconstitution in pre-formed membranes is to insert them readily with the lipid. In contrast to stepwise insertion in the case of preformed membranes, here only a total conductance is recording, and evidence of single channel conductance is not straightforward. Moreover, the presence of lipids might cause denaturation, and additional tests on the functionality should be performed. In addition, each protein requires an optimization with respect to salt, detergent, protein concentration, temperature or incubation time^{12,25–30}.

▲ **CRITICAL** Direct channel reconstitution of proteins into extremely small bilayer is not effective¹². In this case, reconstitution into giant vesicles seems to facilitate the chances for successful reconstitution.

Additional Materials

Lipids dissolved in trichloromethane (5 or 10 mM DPhPC with 10 mol% cholesterol)
Cholesterol, sorbitol and Biobeads
Vesicle Prep Pro (Nanion Technologies)

Procedure

Formation of GUVs:

1. Deposit the solution of lipids dissolved in trichloromethane (20 μ l) on the conductive side of one of the ITO glass supports serving as electrodes.
2. After evaporation, the dried lipid film should result in a clear deposition on the ITO glass slide. After evaporation, place an O-ring with vacuum grease (alternatively a polydimethylsiloxane spacer) around the lipid assembled in a perfectly dehydrated film.
3. To avoid conductance between the glass plates, add salt-free or very low salt solution (1 M sorbitol) to fill the spacer.
4. Place the second ITO glass slide on the top to connect both conductive sides of the respective glass slide.
5. The process of electroformation of GUVs is controlled by empirically optimized parameters (amplitude and frequency of the applied field, time and temperature, concentration of the lipid). The use of the Vesicle Pro for the electroswelling allows one to benefit from the use of its software. Typically, an alternating voltage of 3 V/10 Hz or less (peak to peak), with a progressive increase at the beginning of the protocol and a progressive decrease at the end of the protocol, is applied for ~2 h, resulting in vesicle sizes varying from 5 to 100 μ m.

■ **PAUSE POINT** Vesicles can be stored for a few days.

6. Test these GUVs by performing Step 1D of the PROCEDURE.

Reconstitution of the membrane protein into GUVs:

7. Add solubilized proteins in detergent (e.g., OmpF (1 mg/ml) in OPOE (1 wt%)) to the solution containing GUVs (in 1 M sorbitol; 0.2 μ l of proteins in 270 μ l of GUV solution)¹².
8. Incubate the mix at room temperature for 15 min to 30 min.
9. Add Bio-beads (15–40 mg of dry weight per milliliter) to remove the detergent, and allow the mixture incubate overnight at 4 °C.
10. Briefly centrifuge the Bio-beads and remove the beads.
11. Use the GUVs for recordings (Step 1D of the PROCEDURE).

? TROUBLESHOOTING

■ **PAUSE POINT** GUVs are stable over long periods of time (a few days to a few weeks) at 4 °C.

- (vii) Proteo-GUVs prepared as described in **Box 2** can be used directly for lipid bilayer formation on the pipette tips, and they allow for single-channel recordings^{12,41,42}. Add the solution containing (proteo)-GUVs in the measurements buffer—typically 10 μ l—to the bath solution. Note that the number of vesicles may vary from batch to batch.
- (viii) Apply suction to the back of the nanopipette by means of a simple syringe. There is no need to carefully control the pressure, as our empirical findings suggest that the pressure does not need to be carefully controlled for bilayer formation. By using the unmodified borosilicate glass nanopipettes, bilayers can be reliably formed in a broad range of salt concentrations (250 mM–1 M) and at different pH values (6–8), although success rates tend to be higher at the lower end of the given pH range.
- (ix) Constantly monitor the ionic current after the addition of the GUVs. This should be performed at low voltages of 10 mV. A drop in current signals the formation of the bilayers. For plain GUVs, one should observe resistance increases by several orders of magnitude, possibly up to several hundred gigaohms. For proteo-GUVs, one observes either a finite conductance indicating the presence of a protein channel such as the porin OmpF in the membrane or a plain bilayer. If the bilayer from the proteo-GUVs does not contain the desired number of protein channels, break the bilayer by simply applying 1 V and positive pressure to remove it. Form the next bilayer directly afterward in a matter of seconds by reversing the pressure. This procedure allows for a high turnover and sampling tens of proteo-GUVs in a few minutes. If bilayers do not form anymore, add more proteo-GUVs; if this does not help, exchange the nanopipette and start over.

● **TIMING**

Step 1A, solvent-containing membranes (Mueller-Rudin): 1–2 h

Step 1B, solvent-free membranes (Montal-Mueller): 1–2 h

Step 1C, variation of the Montal-Mueller procedure to prepare asymmetric membranes: 1–2 h

Step 1D, formation of free-standing lipid bilayers on glass nanopipettes: 1–2 h

Box 1, protein reconstitution into planar membranes: 30 min

Box 2, GUV formation and reconstitution of membrane proteins into giant vesicles for patch clamping: 1–2 h

? **TROUBLESHOOTING**

Step 1A

The aim in Step 1A is to form an extremely stable membrane. This is characterized by having a low capacitance and low noise at higher transmembrane voltages.

Too much pre-painting in Step 1A(i) favors a blob formation. If this happens, the cuvette needs to be cleaned and dried again.

More stable membranes can be achieved by replacing the lipid by block co-polymer⁴³. Alternatively, hydrophobic monomers of a polymerizable molecule can be added to the membrane-forming solution. After the formation of a lipid membrane is completed, the active monomers in the solvent can be polymerized⁴⁴. All these approaches allow extremely stable membrane formation resisting 1 V transmembrane potentials⁴⁵.

Step 1B

Problem: membrane does not form.

Possible cause and solution: in Step 1B(iv), the aperture should be free of excess hexadecane; if it becomes blocked, the hexadecane can be removed by gently pipetting the solution at the aperture. It is important to note that an air bubble can block small apertures (<40 μ m).

Protein reconstitution (Box 1)

Problem: protein reconstitution does not proceed as expected (i.e., no detectable increase in conductance, random flickering, rupture of the membrane).

Possible cause and solution: repeated protein addition brings substantial amounts of detergent inside. This reduces the chance for protein reconstitution, and it may cause detergent pore formation. This requires restarting the procedure from the beginning.

Formation of GUVs and reconstitution of membrane proteins into giant vesicles for patch clamping (Box 2, step 11)

Problem: no bilayers form.

Solution: begin by removing the nanopipette from the bath solution to remove residual lipids. If this does not help, try changing the nanopipette. If the last step fails, clean everything and make new GUVs, as it is probable that the GUV batch was not good anymore.

PROTOCOL

Problem: bilayers are not stable.

Solution: make new GUVs; try changing the cholesterol concentration in the GUVs. If this does not work, change the opening diameter of the nanopipette to adjust the stability of the bilayers.

Problem: no flow through the nanopipette.

Solution: increase the diameter by adapting your pulling program.

Problem: no channel activity.

Solution: for proteo-GUVs, increase the concentration of channels during formation. For channel reconstitution, e.g., for α -hemolysin, increase the monomer concentration in the bath, or change the bilayer or batch of proteins⁴⁶. For the reconstitution experiments, check that you are flushing the bath solution before adding the protein, as otherwise the protein will insert into the GUVs in the bath and not into the bilayer on the nanopipette tip.

ANTICIPATED RESULTS

Potential pore size

A typical question is about the pore size of an unknown protein channel. For this, we recommend to start with the formation of a solvent-containing membrane (Step 1A). The addition of protein (**Box 1**) causes a stepwise increase in membrane conductance (**Fig. 2e**). Each step is interpreted as insertion of one (or more) function unit, which may be monomers or oligomers. Plotting the probability of the occurring conductance steps results in a distribution around one and at multiples of the unit-conductance value. In order to get statistically meaningful results, we usually count >100 protein insertions accumulated over several membranes and, if possible, several membrane protein preparations^{47,48}.

Note that if the protein of interest has been expressed in cell-free extracts or in *E. coli*, the reagent solution might contain some OmpF trimer as a contaminant. OmpF is known for its outstanding stability and rapid membrane insertion. In case of doubt (e.g., if you see similar conductances, e.g., 4 nS at 1 M KCl or gating at ~130 mV), we recommend titrating the solution with micromolar concentrations of enrofloxacin⁴⁹. Enrofloxacin is an antibiotic that enters the bacteria through OmpF, and it has a specific affinity and results in specific complete inhibition of OmpF's over a few milliseconds. This inhibition is very specific, and it disappears in the presence of divalent salts, e.g., MgCl₂.

The interpretation of pore size on the basis of the conductance steps is nontrivial. First, to avoid any specific ion interaction, the above approach has to be repeated at two or three different salt concentrations (10 mM to 1 M) and for different cations and anions. In a first-order approximation, the channel is treated as a noninteracting cylinder, and thus the conductance $G = \kappa A/d$, where κ is the bulk conductance, A is the area of the pore and d is the thickness. The latter is usually assumed to be ~4 nm for a porin channel, corresponding to the hydrophobic thickness of the membrane^{23,50}. Obviously, this is only a zero-order approximation that provides adequate results in the absence of any structural information. Refinement has been suggested; titration at low salt concentration gives some hints about the possible surface charges inside the channel, and size exclusion with polymers that are unable to penetrate the channel because of their size gives some further hint about steric exclusion and thus a further hint on possible sizes⁵¹. Overall, such information is very limited despite numerous theoretical attempts at improvement. The possibility of having a high-resolution structure combined with all-atom modeling now allows a parameter-free interpretation of conductance values^{52,53}.

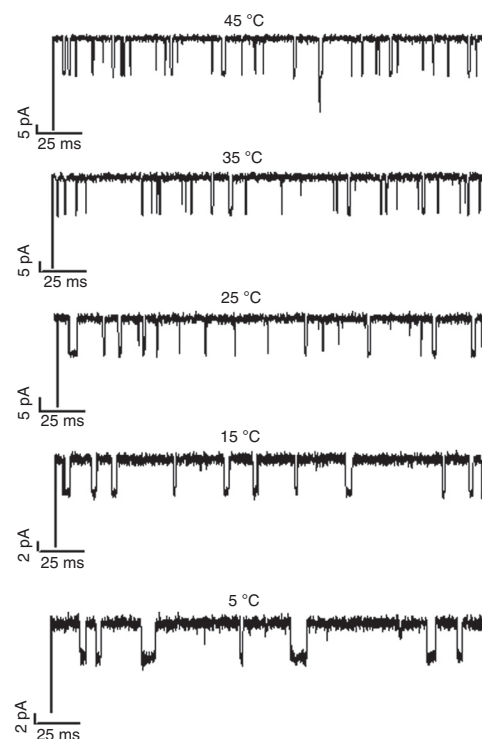
Selectivity

To elucidate ion selectivity, we reconstitute the channels according to one of the procedures described above. Selectivity describes the kinetics of ion permeation, and it is thus not an equilibrium measurement^{54,55}. Moreover, the selectivity is set by the interaction of the ion with the channel interior, and thus it depends on the type and concentration of the salt. Selectivity as given by the permeability ratio of cation/anions is not a universal value, but it depends on the exact experimental condition. A detailed discussion could be found in a serial investigation by Aguilera and co-workers⁵⁵. Typically, a tenfold ion concentration gradient (100 mM/1 M) is applied and with different permeabilities leading to an increased number of ion species with respect to the counter ion leading. This gives rise to a transmembrane potential, which is usually interpreted using the Goldman-Hodgkin-Katz equation. Note that the selectivity or the permeability ratio depends on the salt concentration and on the ion concentration gradient. Furthermore, the potential at the electrode-electrolyte interface depends on the salt concentration, and salt bridges are required to balance this contribution. Special care has to be taken with respect to the definition of the reversal potential²³. Again, the availability of a high-resolution structure allows all-atom modeling, which gives an atomistic view of molecular selectivity⁵⁶.

Substrate binding

The original suggestion to reveal substrate binding using electrophysiology was introduced in an earlier work by Benz and co-workers^{9,56,57}. By following the protocol Step 1A, a few hundred LamB (Maltoporin) channels were reconstituted. The rate

Figure 5 | Reconstitution of a single trimeric maltoporin channel into a virtually solvent-free planar lipid bilayer and application of -150 mV transmembrane voltage cause an ion current. For example, the presence of sugar (here maltohexaose at 2.5 μ M) causes short interruptions of the ion current. Statistical analysis of these blockages allows conclusion on the mode of permeation into the channel. Here we show typical temperature dependence in the range of 5 – 45 $^{\circ}$ C in 1 M KCl at pH 6.



of reconstitution slows down and reaches saturation within an hour. The addition of malto-oligosaccharides reduces the conductance in a concentration-dependent manner. In this study, the binding constant for oligosaccharides was obtained by noting at what point the substrate concentration caused the conductance to be reduced to half of the original value. Later noise analysis of the ion current in the presence of substrate allowed the calculation of the kinetic rate for sugar entry and exit.

When performing analyses at a single-channel level (solvent-free membranes), individual blockages can be observed (Fig. 5; refs. 9,24,25,58). Note that these measurements are indirect measurements, and they do not allow direct conclusion on permeation⁴⁹. Again, all-atom modeling based on a high-resolution structure provides details about potential transport.

Techniques and problems

The conductance of lipid channels observed by the patch technique is often difficult to reproduce quantitatively. In contrast, channel proteins that are overexpressed in cells typically display a well-defined conductance. One likely source of uncertainty is membrane curvature induced by slight pressure differences across the membrane patch. Owing to the small diameter of the pipette tip, curvatures are putatively much higher than in the BLM technique. Membranes with a radius of curvature of 3 μ m (not unreasonable for a pipette tip with a diameter of 1 μ m) can cause a trans-membrane voltage of the order of 100 mV owing to a phenomenon called flexo-electricity, whereas a radius of curvature of 40 μ m or larger expected for BLMs causes voltages of <7 mV (ref. 59). Probably for this reason, the current-voltage relations of BLMs are typically symmetric in voltage in contrast to those for pipette patches, in which they are often asymmetric or rectified^{33,34}. Thus, outward or inward rectified currents are not exclusive for protein channels, and therefore they cannot serve as a reliable fingerprint for a protein channel. To make experiments reproducible, it seems necessary to control the exact pressures on the two sides of the membrane patch, as well as the size of the pipette tip.

It is important to note that proteins are likely to be able to catalyze lipid membrane conductance. This makes it difficult to design good controls that can help distinguish between protein and lipid channels. The experiment itself does not tell the exact location of a conduction event. It is possible that the two phenomena are often confused in the literature, that they are strongly correlated or that they are not different at all. Thus, in biological membranes, it is safest and probably thermodynamically more meaningful to consider conduction events as properties of lipid-protein ensembles.

ACKNOWLEDGMENTS The research leading to these results was conducted as part of the Translocation consortium, and it has received support from the Innovative Medicines Joint Undertaking under grant agreement no. 115525, resources which are composed of financial contributions from the EU's seventh framework program (FP7/2007-2013) and European Federation of Pharmaceutical Industries and Associations (EFPIA) companies' in-kind contribution, as well as grant no. Wi2278/18-1 from the Deutsche Forschungsgemeinschaft (DFG). U.K. acknowledges funding from a European Research Council starting grant.

AUTHOR CONTRIBUTIONS All authors contributed equally to manuscript writing.

COMPETING FINANCIAL INTERESTS The authors declare no competing financial interests.

Reprints and permissions information is available online at <http://www.nature.com/reprints/index.html>.

1. Benz, R., Janko, K., Boos, W. & Lauger, P. Formation of large, ion-permeable membrane channels by the matrix protein (porin) of *Escherichia coli*. *Biochim. Biophys. Acta* **511**, 305–319 (1978).
2. Luckey, M. & Nikaido, H. Diffusion of solutes through channels produced by phage λ receptor protein of *Escherichia coli*: inhibition by higher oligosaccharides of maltose series. *Biochem. Biophys. Res. Commun.* **93**, 166–171 (1980).
3. Nikaido, H. Porins and specific channels of bacterial outer membranes. *Mol. Microbiol.* **6**, 435–442 (1992).
4. Sakmann, B. & Neher, E. in *Single-Channel Recordings* (Plenum Press, 1983).
5. Mueller, P., Rudin, D.O., Tien, H.T. & Wescott, W.C. Reconstitution of cell membrane structure *in vitro* and its transformation into an excitable system. *Nature* **194**, 979–980 (1962).
6. Montal, M. & Mueller, P. Formation of bimolecular membranes from lipid monolayers and a study of their electrical properties. *Proc. Natl. Acad. Sci. USA* **69**, 3561–3566 (1972).

7. Neher, E. & Sakmann, B. Single-channel currents recorded from membrane of denervated frog muscle fibres. *Nature* **260**, 799–802 (1976).
8. Montal, M., Darszon, A. & Schindler, H.G. Functional reassembly of membrane proteins in planar lipid bilayers. *Q. Rev. Biophys.* **14**, 1–79 (1981).
9. Nekolla, S., Andersen, C. & Benz, R. Noise analysis of ion current through the open and the sugar-induced closed state of the LamB channel of *Escherichia coli* outer membrane: evaluation of the sugar binding kinetics to the channel interior. *Biophys. J.* **66**, 1388–1397 (1994).
10. Hagge, S.O. *et al.* Pore formation and function of phosphoporphin PhoE of *Escherichia coli* are determined by the core sugar moiety of lipopolysaccharide. *J. Biol. Chem.* **277**, 34247–34253 (2002).
11. Wilmsen, U., Methfessel, C., Hanke, W. & Boheim, G. in *Physical Chemistry of Transmembrane Ion Motions* (ed. Troyanowsky, C.) (Elsevier, 1983).
12. Gornall, J.L. *et al.* Simple reconstitution of protein pores in nano lipid bilayers. *Nano Lett.* **11**, 3334–3340 (2011).
13. Schmidt, C., Mayer, M. & Vogel, H. A chip-based biosensor for the functional analysis of single ion channels. *Angew. Chem. Int. Ed.* **39**, 3137–3140 (2000).
14. Dilger, J.P. & Benz, R. Optical and electrical properties of thin monoolein lipid bilayers. *J. Membr. Biol.* **85**, 181–189 (1985).
15. Bähr, G., Diederich, A., Vergères, G. & Winterhalter, M. Interaction of the effector domain of MARCKS and MARCKS-related protein with lipid membranes revealed by electric potential measurements. *Biochemistry.* **37**, 16252–16261 (1998).
16. Hagge, S.O., Wiese, A., Seydel, U. & Gutschmann, T. Inner field compensation as a tool for the characterization of asymmetric membranes and peptide-membrane interactions. *Biophys. J.* **86**, 913–922 (2004).
17. Coronado, R. & Latorre, R. Phospholipid bilayers made from monolayers on patch-clamp pipettes. *Biophys. J.* **43**, 231–236 (1983).
18. Hanke, W., Methfessel, C., Wilmsen, U. & Boheim, G. Ion channel reconstitution into lipid bilayer-membranes on glass patch pipettes. *Bioelectrochem. Bioenerget.* **12**, 329–339 (1984).
19. Sondermann, M., George, M., Fertig, N. & Behrends, J.C. High-resolution electrophysiology on a chip: transient dynamics of alamethicin channel formation. *Biochim. Biophys. Acta* **1758**, 541–551 (2006).
20. White, R.J. *et al.* Single ion-channel recordings using glass nanopore membranes. *J. Am. Chem. Soc.* **129**, 11766–11775 (2007).
21. Schibel, A.E.P., Edwards, T., Kawano, R., Lan, W. & White, H.S. Quartz nanopore membranes for suspended bilayer ion channel recordings. *Anal. Chem.* **82**, 7259–7266 (2010).
22. Goepfrich, K., Kulkarni, C.V., Pambos, O. & Keyser, U.F. Lipid nanobilayers to host biological nanopores for DNA translocations. *Langmuir* **29**, 355–364 (2013).
23. Danelon, C., Suenaga, A., Winterhalter, M. & Yamato, I. Molecular origin of the cation selectivity in OmpF porin: single channel conductances vs. free energy calculation. *Biophys. Chem.* **104**, 591–603 (2003).
24. Orlik, F., Andersen, C., Danelon, C., Winterhalter, M., Pajatsch, M., Böck, A. & Benz, R. CymA of *Klebsiella oxytoca* outer membrane: binding of cyclodextrins and study of the current noise of the open channel. *Biophys. J.* **85**, 876–885 (2003).
25. Danelon, C., Brando, T. & Winterhalter, M. Probing the orientation of reconstituted maltoporin channels at the single-protein level. *J. Biol. Chem.* **278**, 35542–35551 (2003).
26. Schwarz, G., Danelon, C. & Winterhalter, M. On translocation through a membrane channel via an internal binding site: kinetics and voltage dependence. *Biophys. J.* **84**, 2990–2998 (2003).
27. Mahendran, K.R., Chimere, C., Mach, T. & Winterhalter, M. Antibiotic translocation through membrane channels: temperature dependent ion current fluctuation for catching the fast events. *Eur. Biophys. J.* **38**, 1141–1145 (2009).
28. Mahendran, K.R., Lamichhane, U., Romero-Ruiz, M., Nussberger, S. & Winterhalter, M. Polypeptide translocation through mitochondrial TOM channel: temperature dependent rates at single molecule level. *J. Phys. Chem. Lett.* **4**, 78–82 (2013).
29. Singh, P. *et al.* Pulling peptides across nanochannels: resolving peptide binding and translocation through the hetero-oligomeric channel from *Nocardia farcinica*. *ACS Nano* **6**, 10699–10707 (2012).
30. Brauser, A. *et al.* Modulation of enrofloxacin binding in OmpF by Mg²⁺ as revealed by the analysis of fast flickering single-porin current. *J. Gen. Physiol.* **140**, 69–82 (2012).
31. Laub, K.R. *et al.* Comparing ion conductance recordings of synthetic lipid bilayers with cell membranes containing TRP channels. *Biochim. Biophys. Acta* **1818**, 1123–1134 (2012).
32. Antonov, V., Petrov, V., Molnar, A., Predvoditelev, D. & Ivanov, A. The appearance of single-ion channels in unmodified lipid bilayer membranes at the phase transition temperature. *Nature* **283**, 585–586 (1980).
33. Heimburg, T. *Thermal Biophysics of Membranes* (Wiley-VCH, Weinheim, 2007).
34. Heimburg, T. Lipid ion channels. *Biophys. Chem.* **150**, 2–22 (2010).
35. Mosgaard, L.D. & Heimburg, T. Lipid ion channels and the role of proteins. *Acc. Chem. Res.* **46**, 2966–2976 (2013).
36. Blicher, A. & Heimburg, T. Voltage-gated lipid ion channels. *PLoS ONE* **8**, e65707 (2013).
37. Lindey, H., Petersen, N.O. & Chan, S.I. Physicochemical characterization of 1,2-diphytanoyl-sn-glycero-3-phosphocholine in model membrane systems. *Biochim. Biophys. Acta* **555**, 147–167 (1979).
38. Brullemans, M. & Tancrede, P. Influence of torus on the capacitance of asymmetrical phospholipid bilayers. *Biophys. Chem.* **27**, 225–231 (1987).
39. Wolfe, A.J., Mohammad, M.M., Cheley, S., Bayley, H. & Movileanu, L. Catalyzing the translocation of polypeptides through attractive interactions. *J. Am. Chem. Soc.* **129**, 14034–14041 (2007).
40. Angelova, M.I. & Dimitrov, D.S. Liposome electroformation. *Faraday Disc.* **81**, 303–311 (1986).
41. Burn, J.R. *et al.* Lipid-bilayer-spanning DNA nanopores with a bifunctional porphyrin anchor. *Angew. Chem. Int. Ed.* **52**, 12069–12072 (2013).
42. Holden, M.A., Jayasinghe, L., Daltrop, O., Mason, A. & Bayley, H. Direct transfer of membrane proteins from bacteria to planar bilayers for rapid screening by single-channel recording. *Nat. Chem. Biol.* **2**, 314–318 (2006).
43. Nardin, C., Winterhalter, M. & Meier, W. Giant free standing films from ABA triblock copolymer. *Langmuir* **16**, 7708–7712 (2000).
44. Meier, W., Graff, A., Diederich, A. & Winterhalter, M. Stabilization of planar lipid membranes. *Phys. Chem. Chem. Phys.* **2**, 4559–4562 (2000).
45. Winterhalter, M. Lipid membranes in external electric fields: kinetics of large pore formation causing rupture. *Adv. Colloid Interface Sci.* **208**, 121–128 (2014).
46. Schuster, B., Pum, D., Braha, O., Bayley, H. & Sleytr, U.B. Self-assembled α -hemolysin pores in an S-layer-supported lipid bilayer. *Biochim. Biophys. Acta* **1370**, 280–288 (1998).
47. van der Woude, A.D. *et al.* Differential detergent extraction of mycobacterium marinum cell envelope proteins identifies an extensively modified threonine-rich outer membrane protein with channel activity. *J. Bacteriol.* **195**, 2050–2059 (2013).
48. Mafakheri, S. *et al.* Discovery of a cell wall porin in the mycolic-acid-containing actinomycete *Dietzia maris* DSM 43672. *FEBS J.* **281**, 2030–2041 (2014).
49. Mahendran, K. *et al.* Molecular basis of enrofloxacin translocation through a bacterial porin: when binding does not imply translocation. *J. Phys. Chem. B* **114**, 5170–5179 (2010).
50. Mahendran, K.R. *et al.* Permeation through nanochannels: revealing fast kinetics. *J. Phys. Condens. Matter* **22**, 454131 (2010).
51. Krasilnikov, O.V., Sabirov, R.Z., Ternovsky, V.I., Merzliak, P.G. & Tashmukhamedov, B.A. The structure of *Staphylococcus aureus* α -toxin-induced ionic channel. *Gen. Physiol. Biophys.* **7**, 467–473 (1988).
52. Chimere, C., Movileanu, L., Pezeshki, S., Winterhalter, M. & Kleinekathöfer, U. Transport at the nanoscale: temperature dependence of ion conductance. *Eur. Biophys. J.* **38**, 121–125 (2008).
53. Modi, N., Winterhalter, M. & Kleinekathöfer, U. Computational modeling of ion transport through nanopores. *Nanoscale* **4**, 6166–6180 (2012).
54. Hille, B. *Ion Channels of Excitable Membranes* (Sunderland, 2001).
55. Lopez, M.L., Garcia-Gimenez, E., Aguilera, V.M. & Alcaraz, A. Critical assessment of OmpF channel selectivity. *J. Phys. Condens. Matter* **22**, 454106 (2010).
56. Pezeshki, S., Chimere, C., Bessonov, A.N., Winterhalter, M. & Kleinekathöfer, U. Understanding ion conductance on a molecular level: an all-atom modeling of the bacterial porin OmpF. *Biophys. J.* **97**, 1898–906 (2009).
57. Benz, R., Schmid, A., Nakae, T. & Vos-Scheperkeuter, G.H. Pore formation by LamB of *Escherichia coli* in lipid bilayer membranes. *J. Bacteriol.* **165**, 978–986 (1986).
58. Bezrukov, S.M. & Winterhalter, M. Examining noise sources at the single-molecule level: 1/f noise of an open maltoporin channel. *Phys. Rev. Lett.* **85**, 202–205 (2000).
59. Petrov, A.G. Flexoelectricity of model and living membranes. *Biochim. Biophys. Acta* **1561**, 1–25 (2001).
60. Lamichhane, U. *et al.* Peptide translocation through mesoscopic channel: binding kinetics at single-molecule level. *Eur. Biophys. J.* **42**, 363–369 (2013).
61. Morandot, S. & El Kirat, K. Solubilization of supported lipid membranes by octylglucoside observed by time-lapse atomic force microscopy. *Colloid Surf. B* **55**, 179–184 (2007).
62. Rigaud, J.L., Levy, D., Mosser, G. & Lambert, O. Detergent removal by non-polar polystyrene beads. *Eur. Biophys. J.* **27**, 305–319 (1998).